

Estimating the transfer function of the cantilever in atomic force microscopy: A system identification approach

Martin Stark

*Max-Planck-Institut für Biochemie, 82152 Martinsried, Germany
and Ecole Polytechnique Fédérale de Lausanne, Institut des Sciences et Ingénierie Chimiques,
Laboratory of Ultrafast Laser Spectroscopy, 1015 Lausanne, Switzerland*

Reinhard Guckenberger

Max-Planck-Institut für Biochemie, 82152 Martinsried, Germany

Andreas Stemmer

*Swiss Federal Institute of Technology Zurich, Nanotechnology Group, ETH Zentrum CLA,
8092 Zurich, Switzerland*

Robert W. Stark^{a)}

*Swiss Federal Institute of Technology Zurich, Nanotechnology Group, ETH Zentrum CLA,
8092 Zurich, Switzerland
and Ludwig-Maximilians-Universität München, Crystallography, Theresienstrasse 41,
80333 Munich, Germany*

(Received 17 May 2005; accepted 18 October 2005; published online 7 December 2005)

Dynamic atomic force microscopy (AFM) offers many opportunities for the characterization and manipulation of matter on the nanometer scale with a high temporal resolution. The analysis of time-dependent forces is basic for a deeper understanding of phenomena such as friction, plastic deformation, and surface wetting. However, the dynamic characteristics of the force sensor used for such investigations are determined by various factors such as material and geometry of the cantilever, detection alignment, and the transfer characteristics of the detector. Thus, for a quantitative investigation of surface properties by dynamic AFM an appropriate system identification procedure is required, characterizing the force sensor beyond the usual parameters spring constant, quality factor, and detection sensitivity. Measurement of the transfer function provides such a characterization that fully accounts for the dynamic properties of the force sensor. Here, we demonstrate the estimation of the transfer function in a bandwidth of 1 MHz from experimental data. To this end, we analyze the signal of the vibrations induced by snap-to-contact and snap-off-contact events. For the free cantilever, we determine both a parameter-free estimate [empirical transfer function estimate (ETF)] and a parametric estimate of the transfer function. For the surface-coupled cantilever the ETF is obtained. These identification procedures provide an intrinsic calibration as they dispense largely with *a priori* knowledge about the force sensor. © 2005 American Institute of Physics. [DOI: [10.1063/1.2137887](https://doi.org/10.1063/1.2137887)]

INTRODUCTION

For a quantitative and time-resolved surface analysis by dynamic atomic force microscopy (AFM) exact knowledge of the frequency response characteristics of the force sensor is required. System identification methods¹ provide a powerful toolbox to characterize the dynamic response from experimental stimulus-response data. A full spectral characterization of the AFM system allows for a virtual real-time representation of AFM experiments,² for fast and efficient dynamic control,^{3,4} for nanorobotics,^{5,6} and for time-resolved force measurements.^{7,8} Similarly, recent advances in dynamic AFM techniques such as electrostatic force microscopy⁹ multifrequency force spectroscopy,¹⁰ and acoustic atomic force microscopy,^{11–13} demand characterization tools adapted to broadband measurements. Furthermore,

such a broadband characterization can help us to analyze data obtained by dynamic force spectroscopy,^{14,15} where the nonlinear interaction forces generate higher harmonics of the driving frequency.^{16,17}

In a typical calibration procedure the static relation between the cantilever deflection and the photodiode signal has to be determined. The lever sensitivity is usually estimated from data of force-curve experiments on hard substrates. The spring constant is the second key parameter that has to be determined. For this purpose various methods can be used. Among the most common techniques there are the thermal noise method,^{18–21} the added mass method,²² the method of Sader *et al.*,²³ and calibration procedures employing a reference spring.^{24–26} The system resonances²⁷ as well as the mechanical impedance in the frequency range below 100 kHz (Ref. 28) were determined for a dynamic characterization of the cantilever by external excitation.

The force sensor can be well understood as a nonmonotonous mechanical filter.^{29,30} Essentially, the structure in

^{a)} Author to whom correspondence should be addressed; FAX: +49 89 2180 4334; electronic mails: stark@nanomanipulation.de and stark@lrz.uni-muenchen.de

this filter's frequency response is related to cantilever properties, to the type and the actual adjustment of the detection, and to the coupling of the typical force load, such as distributed load, base excitation, or pointlike load at the tip. After measuring the spring constant and optical lever sensitivity one has to determine the spectral response of the force sensor. Technically, the main difficulty is to apply a defined force at the tip location that corresponds to a point load.

The system theory provides a convenient formalism to describe the relation between the force input and the measured signal output. In the Laplace domain with the Laplace variable $s=j\omega$ the continuous transfer function of the force sensor is defined by

$$G(s) = \frac{y(s)}{u(s)}. \quad (1)$$

This characterizes the relation between the force sensor output $u(s)$ and the input force acting on the tip $y(s)$. The transfer function can be approximated theoretically assuming an infinite dimensional system,^{31,32} a truncated model,^{27,29} or by a discrete approximation.³³

The application of theoretical models to the analysis of experimental data is hampered by significant deviations from the idealized geometry and difficulties due to the finite spot size of the detection laser.^{34,35} More importantly, the transfer function critically depends on the adjustment of the optical deflection readout.³⁶ This means that the transfer function has to be estimated from experimental data, since theoretical models may fail to provide a model with the required accuracy.

In the following, we report on the experimental estimation of the transfer function of a cantilever force sensor used in AFM. The need for *a priori* knowledge is reduced by system intrinsic measurements that are based on the analysis of discontinuous events in standard force-displacement curves. For the free and the surface-coupled cantilever the empirical transfer function estimate (ETFE) is obtained as a parameter-free estimate. Additionally, we calculate a parametric estimate for the free cantilever employing a black-box system identification algorithm. Both estimation procedures are based on the analysis of the time series data acquired during a static force spectroscopy experiment. We suggest analyzing the time series data following a snap-off-contact event in order to estimate the transfer function of the free cantilever. Similarly, the snap-to-contact event may be employed to extract the characteristics of the surface-coupled cantilever.

THEORETICAL BACKGROUND

Overview

Figure 1 sketches the AFM cantilever in interaction with the sample surface and the corresponding representation as a dynamic system with an output feedback.^{7,29,37} While the forces between tip and sample play the role of a nonlinear output feedback (lower branch) the signal formation branch itself is modeled as a linear time-invariant system (upper branch). The experimentally relevant signal path in Fig. 1(a)

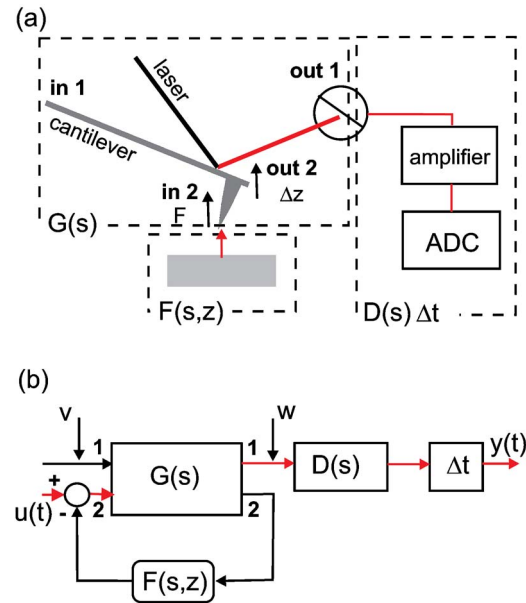


FIG. 1. (Color online) (a) Scheme of an AFM and (b) the description by a dynamic system. The cantilever is modeled as the linear time-invariant system $G(s)$. The forces acting on the tip (input 2) and the external driving (input 1) are system inputs, whereas the tip deflection z and the photodiode signal are system outputs. The nonlinear tip-sample forces $F(s,z)$ are treated as a nonlinear output feedback. The photodiode electronics is included as a separate system $D(s)$. The data acquisition can also lead to a time delay Δt . In addition, process noise ν and measurement noise w may be present.

leads from the tip-sample forces (input 2) to the sensor readout (output 1) described by the transfer function of the entire signal path [Fig. 1(b)]

$$P(s) = G_{21}(s)D(s)\exp(-s\Delta t) \quad (2)$$

that also includes a time delay $\exp(-s\Delta t)$. A time delay can be introduced by analog-to-digital conversion or may be caused by a finite traveling time of a signal from an input to a distant output. Here, input 2 (located at the tip) and output 1 (located at the laser spot) are collocated on the cantilever. Thus, the traveling time of the mechanical wave from input 2 to output 1 can be neglected. In the following, the time delay accounts for a possible delay during digitalization and for the uncertainty in the determination of the jump-out-of-contact time. For convenience, the transfer function $P(s)$ is split into two components: the rational transfer function,

$$G_D(s) = G_{21}(s)D(s), \quad (3)$$

and the time delay, $\exp(-s\Delta t)$. The transfer function $G_D(s)$ describes the dynamic characteristics of the microcantilever together with the detection system. The time delay is treated as a separate parameter.

In the Laplace domain, the forces between tip and sample $u(s)$ translate into the signal $y(s)$ by

$$y(s) = \frac{k_{\text{ols}}}{k_c} G_D(s)\exp(-s\Delta t)u(s). \quad (4)$$

This equation contains the parameters that have to be determined for a full dynamic calibration: the static (dc) optical lever sensitivity k_{ols} usually obtained from quasistatic force-curve data, the spring constant k_c as obtained by standard

methods, the normalized transfer function $G_D(s)$, and the time delay Δt .

Several types of noise can be distinguished. Force noise can result from fluctuations in the interaction forces. Further process noise ν can be of thermomechanical origin or it can result from noise in the positioning actuator. Possible sources for measurement noise w are manifold. Evident sources are shot noise in the detector, electronic noise in the amplifiers, and the intrinsic noise on the laser intensity. Further, yet important sources concern fluctuations in the optical path. These fluctuations are, e.g., due to thermal gradients and to dust or contaminations on the reflecting surfaces. Thermal gradients play an extremely important role for both drift and noise. They directly affect the adjustment as far as the mechanical loop between laser source, lever, and detector is concerned. Furthermore, thermal gradients may alter the geometry of the optical path, or the refractive index of the medium, which is important in liquids.

For the experimental estimation of the transfer function $G_D(s)$ it is essential to apply a force stimulus to the tip. In this case, forces between tip and sample acting close to the free end couple with nearly equal efficiency to the cantilever. Other stimulating forces may not act directly on the tip or may even be distributed over the structure. Such a distributed load is produced, e.g., by inertial excitation or by applying an electrostatic field between the specimen and the cantilever at a large tip-sample separation. For a distributed load the coupling efficiency is decreased for higher modes because the structure may be partially excited 180° out of phase. Thus, distributed forces have to be accounted for by a system input that is different from the system input for the tip-sample forces. Moreover, a mechanical excitation at the cantilever base, e.g., by the dither piezo, requires precise knowledge of the transfer characteristics of the piezotransducer and the coupling to the cantilever. Additional complications may arise if the actuator and the sensor are noncollocated, as it is the case for a distributed loading in combination with a deflection readout at the free end. This noncollocated configuration can lead to a nonminimum phase behavior above a finite frequency^{31,38} which is not present in the collocated system.

The jump-out-of-contact response of the AFM cantilever $y(t)$ provides a signal that was used to estimate the transfer characteristics of the cantilever. The advantage of this concept is that it dispenses with an external excitation, where the response of the external transducer (e.g., the driving piezo) and its coupling to the cantilever would also have to be determined. In the jump-out-of-contact response, the system input $u(t)$ essentially corresponds to a step function with a negative force $F = -F_{\text{adh}}$ as long as the cantilever is attached to the specimen and $F = 0$ after the rupture event. Thus, initially the cantilever is loaded with a point force that acts on the tip before it is released. At the rupture event, the force load at the tip is zeroed. Thus, the system intrinsic feedback in Fig. 1(b) is switched off for system identification.

Parameter-free estimate

The theoretical background is only briefly recalled here, a detailed treatment can be found in Chapter 6 of Ref. 1. The

basic idea of the parameter-free estimation procedure is the direct application of Eq. (1) in order to calculate $G(s)$ without further physical assumptions. Since the fast Fourier transformation provides an efficient numerical tool for this purpose the transfer function is calculated in the Fourier domain. The Fourier transformed of the discrete system output is

$$Y_N(\omega) = \frac{1}{\sqrt{N}} \sum_{t=1}^N y(t) e^{-i\omega t}, \quad (5)$$

with the time series data $y(t)$ of length N . Correspondingly, the system input is given by

$$U_N(\omega) = \frac{1}{\sqrt{N}} \sum_{t=1}^N u(t) e^{-i\omega t}. \quad (6)$$

In the following we determine the ETFE defined by

$$G_N(e^{i\omega}) = \frac{Y_N(\omega)}{U_N(\omega)}. \quad (7)$$

This definition assumes that $U_N(\omega) \neq 0$ for all $\omega < \omega_{\text{bw}}$. Thus, the ETFE is not defined for frequencies, where $U_N(\omega) = 0$. At those frequencies there is no information on the cantilever dynamics. For a similar reason, the bandwidth limit ω_{bw} was introduced. Above ω_{bw} the information is considered unreliable and thus has to be rejected. The estimate for the transfer function is referred to as empirical since the only assumption is the linearity of the system under test.

Parameter estimation

For control purposes a parametric model of the cantilever dynamics is desirable. To this end a black-box state space model in the innovations form is used that also accounts for noise. This means that in contrast to the physically motivated state space model as discussed in Ref. 29 we do not presuppose a certain physical model structure. For the parameter estimation we assume a discrete model of the system

$$\begin{aligned} x(t + t_s) &= Ax(t) + Bu(t) + Ke(t), \\ y(t) &= Cx(t) + Du(t) + e(t), \end{aligned} \quad (8)$$

which is equivalent to the transfer function description. Process noise w and measurement noise ν are assumed to be white noise and are represented by the innovation $e(t)$ and the Kalman gain K . The innovation e accounts for the noise contributions to $y(t)$, i.e., to signal components that cannot be predicted by the models A , B , C , and D from preceding input u . In this model, matrix A describes the system dynamics as it is related to the system states x and matrix B models the coupling of the input u to the dynamics. Matrix C accounts for the output coupling of the system states x . Matrix D represents possible contributions from a direct feed through from the input u to the output y . The matrix elements may be complex. The Kalman gain models the noise characteristics from the matrices A and C together with covariance matrices accounting for process and measurement noises ν and w . A detailed description can be found in Ref. 1, page 98. In order to obtain the model parameters they have to be

estimated by an appropriate fitting procedure to reproduce the measured input–output relation.

EXPERIMENT

Setup

A series of quasistatic force-retract curves (without excitation of the cantilever) was performed with a Multimode IIIa (Veeco, Santa Barbara, CA, USA) in contact mode on a silicon test substrate. Large rupture forces were obtained by prior contacting the tip to double-sided adhesive tape. The corresponding photodiode signal was directly extracted at the head, preamplified (SR560, Stanford Research, Sunnyvale, CA, USA), and recorded at 5 MS/s (NI PCI-6110S, National Instruments, Austin, TX, USA). Simultaneously, a low-voltage signal proportional to the high voltage applied to the scanning piezo was recorded referencing the displacement. The thermal noise calibration of the cantilever's spring constant (NSCH 11, Silicon-MDT, Moscow, now NSC 11 Micromasch, Tallinn, Estonia) yielded 3.8 ± 0.4 N/m.

During the experiment, the adjustment of the AFM (laser beam, photodetector, and position on the specimen) was conserved. Thermal noise spectra were taken as control to detect possible alterations of the system. Except for a slight variation of the noise level observed alterations remained within the accuracy of the measurement indicating stability over time. The approach-retract procedure was cycled at 5.58 Hz and covered 200 nm in distance. One file contained 3 MS, i.e., 0.6 s. The experimental data were previously used to reconstruct the time-resolved force.⁷ Here, we revisit the data under the focus of system identification in order to validate a parametric model.

Data processing

Ensembles of 84 snap-off events and 89 snap-to-contact events were extracted from the data (Fig. 2) by an iterative correlation averaging. An average rupture event (average snap-to-contact event) was calculated and served as basis for the subsequent analysis. To detect possible drift problems, subensembles (ordered as well as randomized) were created and compared. No significant variations of the correlation coefficients were observed.

The rupture event of the snap-off contact was considered an input force. Extrapolating the signal without force load long after the rupture to the moment of rupture represented zero force. Extrapolating the linear slope before the event, i.e., the adhesion keeping the cantilever at the surface, to the moment of rupture allowed for the estimation of the quasistatic force load culminating at -330 nN at the moment of rupture. The resulting time course of the force load was estimated combining both extrapolations, as shown in Fig. 2(d) together with an enlargement of the averaged snap-off in Fig. 2(c).

The rupture of the polymer in the tip-sample contact at the jump-out-of-contact time t_0 could not be measured directly. Since theoretical models do not predict a time delay in

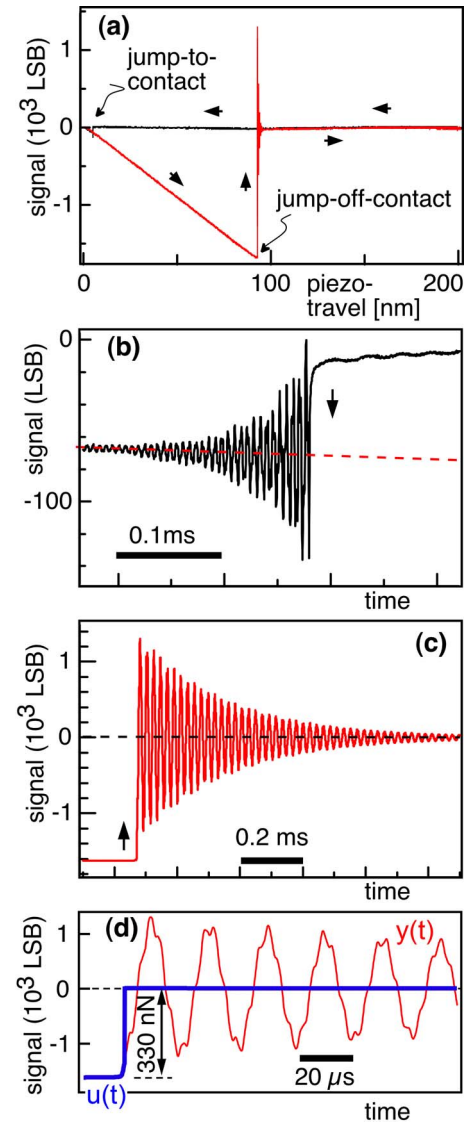


FIG. 2. (Color online) Experimental data. (a) The entire force curve. Details: (b) Oscillations induced by the snap-to-contact event. (c) Oscillations of the free cantilever after snapping off the surface. (d) The averaged oscillations after snap-off (thin line) and the estimate for the tip force (thick line); (1 LSB \approx 0.977 mV).

the mechanical part of the collocated system³¹ the time t_0 was adjusted to the largest possible value compatible with a causal transfer function of the identified system $G_D(s)$. An uncertainty regarding the time delay Δt of about five samples ($\pm 0.5 \mu\text{s}$) remained.

To determine the transfer function of the surface-coupled cantilever the oscillations after the snap-to-contact event were analyzed [Fig. 2(b)]. For the system identification the force was assumed to be zero before the cantilever snapped to the surface. Then, the finite force was increasing linearly with time due to the moving z actuator in contact. Obviously, this procedure includes simplifying assumptions: (i) the surface-coupled cantilever was modeled as a linear system. This neglects the nonlinear tip-sample force after the snap in event. (ii) The simple force model for the system input represents only a rough estimate for the true tip-sample force.

Nevertheless, this procedure allows one to capture qualitatively major features of the dynamics of a surface-coupled cantilever.

For the determination of the ETFE ensembles of events were subsequently processed as follows. Two time series

were obtained by averaging: the signal $y(t)$ that was used as output data and the noise-free estimate of the time course of the corresponding force load $u(t)$. From the averaged time series, $u(t)$ and $y(t)$, $N=8192$ points were selected, respectively. For data preprocessing a Tukey window

$$W(k+1) = \begin{cases} 1.0, & 0 \leq |k| \leq \frac{N}{2}(1+\alpha) \\ 0.5 \left\{ 1.0 + \cos \left[\pi \frac{k - \frac{N}{2}(1-\alpha)}{N(1-\alpha)} \right] \right\}, & \frac{N}{2}(1+\alpha) \leq |k| \leq N \end{cases} \quad (9)$$

with $\alpha=0.1$ was used.

For the *parameter estimation* the ensemble of force curves was randomly split into an identification data set $u_i(t)$ and $y_i(t)$ and a verification data set $u_v(t)$ and $y_v(t)$. A section of $N=8192$ points was selected in all input and output data sets, employing a rectangular window. Data of each set were averaged in order to increase the signal-to-noise ratio. The estimation of the parameters in Eq. (8) was carried out using the graphical user interface of the system identification toolbox of MATLAB 6.5. For the parameter estimation a prediction error/maximum-likelihood method was used [command pem()], which uses a similar algorithm as armax()].

RESULTS AND DISCUSSION

As a first step, the periodograms of the input $U(\omega)$ and the output $Y(\omega)$, which are estimates of the respective power spectral density, were calculated (data not shown). They were computed as the normalized absolute square of the Fourier transform of the corresponding time series. By using Eq. (7) the ETFE G_N was calculated from the windowed data. The dimensionless magnitude was normalized to unity for a quasistatic input. The corresponding Bode plot is shown in Fig. 3 (red). The modal response of the cantilever dynamics prevails as a sequence of resonances and antiresonances (transmission zeros).

The small peak close to the minimum at about 10^5 Hz was accompanied by a phase shift $\Delta\phi = -\pi$. The frequency corresponded to the second harmonic of the fundamental resonance. We assume that a small nonlinearity in the optical detection gave rise to this feature. However, the ETFE is highly reliable at the resonances, while the antiresonances are difficult to be detected due to the low signal level at those frequencies. At that point, appropriate local smoothing routines improve the quality of the ETFE. It is tempting to apply the smoothing directly to amplitude and phase, but this will result in a biased estimate.

This becomes evident by assuming an additional noise spectrum $\phi(\omega)$ due to process and measurement noises. The ETFE is then an asymptotically unbiased estimate of the transfer function $G_D(e^{i\omega})$ with the variance $\phi(\omega)/|U_N(\omega)|^2$. Unfortunately, the expectation value

$$\langle |G_N(e^{i\omega})|^2 \rangle = |G_D(e^{i\omega})|^2 + \frac{\phi(\omega)}{|U_N(\omega)|^2} \quad (10)$$

is biased by $\phi(\omega)/|U_N(\omega)|^2$ for large N .¹ Thus, by smoothing the amplitude response $A(e^{i\omega}) = |G_N(e^{i\omega})|$ one will systematically overestimate the transfer function. In frequency bands with a poor signal-to-noise ratio such as at frequencies close to a transmission zero this would even lead to a systematic error of several orders of magnitude. Instead, any smoothing shall be applied to real and imaginary parts of the ETFE separately, as these are unbiased. Here, we applied local polynomial smoothing to real and imaginary parts of the ETFE. Along with this smoothing procedure the peak at 10^5 Hz was removed from the data. The Bode plot of the smoothed ETFE is displayed in blue in Fig. 3.

By using a similar procedure, the transfer function (ETFE) of the surface-coupled cantilever was obtained. Figure 4 shows the corresponding Bode plot. The measured spectral response is similar to the response predicted by the

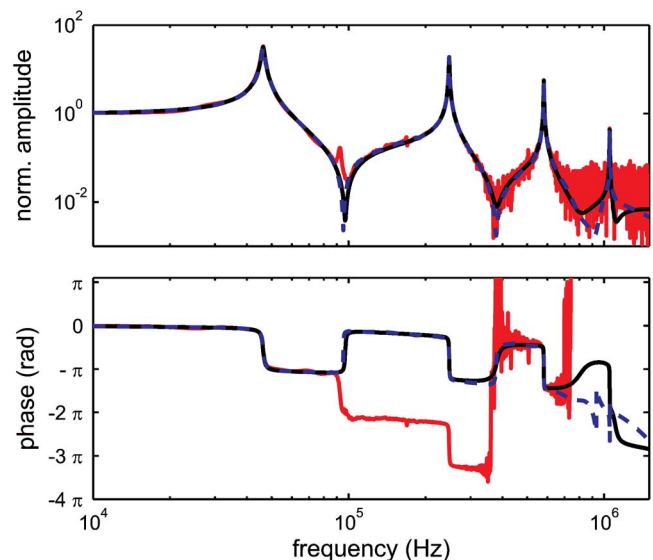


FIG. 3. (Color online) Comparison between ETFE (red), smoothed ETFE (blue, dashed) and an 11th-order parametric estimate (black) of the free cantilever. The response of the smoothed ETFE and the parametric estimate coincides over a wide range of frequencies.

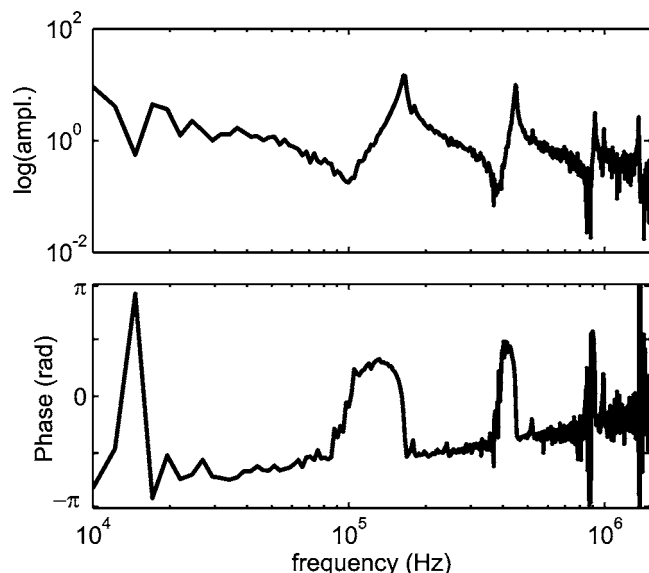


FIG. 4. Bode plot of the empirical transfer function estimate (ETF) for the surface-coupled cantilever as obtained from the jump-to-contact response. The transmission zeros are at the same frequencies as for the free cantilever. The resonances are shifted to higher frequencies as compared to the free cantilever in Fig. 3.

theory:²⁹ a transmission minimum is located below the fundamental resonance. The measured transmission minima are the same as for the free cantilever, whereas the poles (resonances) are shifted to higher frequencies. This can be easily explained by the fact that the zeros of the transfer function depend on the sensor system that was not changed during the experiment, whereas the poles depend on the system intrinsic feedback given by the force coupling of tip and sample. However, the noise level is significantly increased in comparison to the response of the free cantilever as is evident from Fig. 4. Thus, a reliable parameter estimation could not be achieved.

The use of the transfer function of the coupled cantilever for calibration purposes is limited, as it directly depends on the tip-sample interaction. In contrast, the transfer function of the free cantilever is a sensor description that is independent of the interaction force. There, the nonlinear interaction force is considered rather as system-external feedback, i.e., the force acts as input into the system. Thus, describing the surface-coupled cantilever by a linear transfer function means approximating the nonlinear feedback by a linear system, i.e., the force is linearized and considered as system-internal parameter. This is appropriate only in the case of very small oscillatory amplitudes. In all other cases, the system identification problem of the nonlinear closed-loop system (cantilever and sample) requires a mathematical treatment beyond the scope of this study.

For the *parametric characterization* of the free cantilever an 11th-order system was assumed for the model as described by Eq. (8). Lower-order models did not capture relevant features of the cantilever dynamics that were present in the parameter-free estimate. A pole-zero map of the discrete system (sample rate of 5 MS/s) is displayed in Fig. 5. Weakly damped complex conjugate poles correspond to the mechanical resonances of the cantilever whereas the strongly

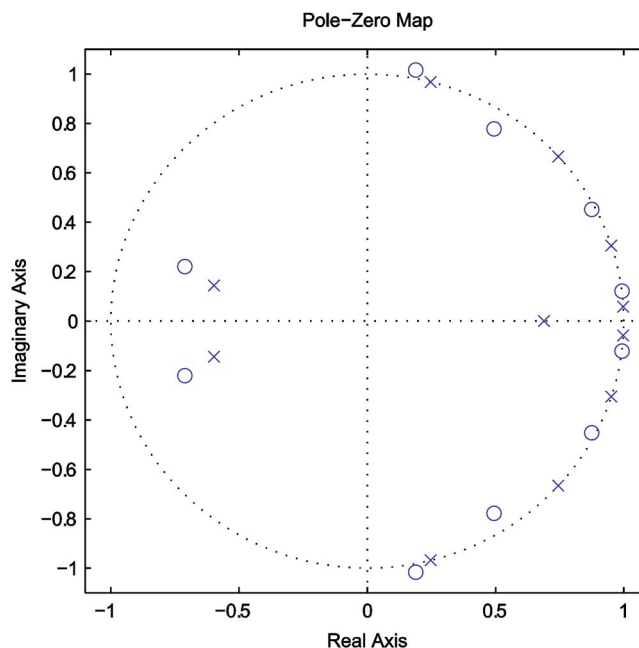


FIG. 5. (Color online) Pole-zero map of the parametric estimate with a sampling rate of 5 MS/s. The weakly damped poles and zeros close to the unit circle correspond to the mechanical characteristics of the cantilever.

damped poles describe the low-pass filter characteristics of the detection system. In order to extract the mechanical characteristics of the cantilever, the discrete system was transformed into a continuous system, $G_D(s)$. The properties of the mechanical system were extracted from the estimated dynamic system and are summarized in Table I. The resonant frequencies obtained by frequency sweep of the excitation frequency well agree with the values that were determined by system identification. In addition, the system identification provides the modal damping. The spectral response as obtained by the system identification is independent from the coupling characteristics of external transducers. In contrast, a resonance curve obtained by a frequency sweep is typically biased by the spectral response of the transducer and the coupling to the force sensor.

A comparison with the parameter-free estimates in Fig. 3 shows that the (smoothed) ETFE well captures the dynamics of the multimodal resonator. Thus, parameter-free methods as well as parameter estimation methods yield a comparable estimate for the transfer function of the free cantilever.

Finally, a limitation of the methodologies as proposed above should be mentioned. The estimation of the transfer characteristics relies on data obtained from the jump-out-of-contact response (jump-to-contact response). Since the time

TABLE I. Summary of the resonant frequencies f_{sweep} and f_{id} . The values were obtained by sweeping the driving frequency and the parameter estimation procedure, respectively. The corresponding modal quality factors are also given.

Flexural mode	1	2	3	4
f_{sweep}	46.2 kHz	247 kHz	581 kHz	1051 kHz
f_{id}	46.3 kHz	247.4 kHz	580.8 kHz	1051.2 kHz
Q_{id}	40.8	193.2	358.0	503.8

evolution of input force is not exactly known, the time delay cannot be estimated from these data. However, by taking into account that the tip-sample forces and the readout are collocated the only time delay to be expected is caused by the detection electronics and the data acquisition.

CONCLUSIONS

Based on the analysis of vibrations after the snap-to-contact and the snap-off events the spectral response of an AFM cantilever can be determined. System identification procedures allow for the determination of parameter-free (ETFE) or parametric estimates. These mathematical models include the dynamic response characteristics of the entire detection system. By analyzing data obtained during an approach-retract cycle, the use of an additional external transducer for the excitation of the cantilever can be completely circumvented.

Procedures to estimate the system transfer function provide an essential input for a real-time reconstruction of tip-sample forces from time series data in dynamic AFM. Moreover, the identification of the parametric transfer characteristics enables the application of advanced signal-processing methods to dynamic AFM such as the design of specialized filters or the use of observers to estimate the evolution of the system state for control purposes. A reliable *in situ* characterization method for the force sensor opens the door for more sophisticated surface analysis and nanomanipulation strategies. One example of such a future development is the extension of the method to a nonlinear system identification procedure of the entire system consisting of the cantilever and the tip-sample interaction. This will allow for the identification of the nonlinear nanomechanical properties of the sample.

ACKNOWLEDGMENT

This work was supported by Top Nano21 under Grant No. 6351.1.

¹L. Ljung, *System Identification: Theory for the User*, 2nd ed. (Prentice-Hall, Upper Saddle River, NJ, 1999).

²G. Couturier, J. P. Aime, J. Salardenne, and R. Boisgard, *Eur. Phys. J.: Appl. Phys.* **15**, 141 (2001).

³T. Sulchek *et al.*, *Appl. Phys. Lett.* **76**, 1473 (2000).

⁴D. R. Sahoo, A. Sebastian, and M. V. Salapaka, *Appl. Phys. Lett.* **83**, 5521 (2003).

⁵M. Guthold *et al.*, *IEEE/ASME Trans. Mechatron.* **5**, 189 (2000).

⁶R. W. Stark, F. J. Rubio-Sierra, S. Thalhammer, and W. M. Heckl, *Eur. Biophys. J.* **32**, 33 (2003).

⁷M. Stark, R. W. Stark, W. M. Heckl, and R. Guckenberger, *Proc. Natl. Acad. Sci. U.S.A.* **99**, 8473 (2002).

⁸B. A. Todd and S. J. Eppell, *J. Appl. Phys.* **94**, 3563 (2003).

⁹H. O. Jacobs, H. F. Knapp, and A. Stemmer, *Rev. Sci. Instrum.* **70**, 1756 (1999).

¹⁰T. R. Rodríguez and R. García, *Appl. Phys. Lett.* **84**, 449 (2004).

¹¹U. Rabe and W. Arnold, *Appl. Phys. Lett.* **64**, 1493 (1994).

¹²E. Dupas, G. Gremaud, A. Kulik, and J. L. Loubet, *Rev. Sci. Instrum.* **72**, 3891 (2001).

¹³M. T. Cuberes, H. E. Assender, G. A. D. Briggs, and O. V. Kolosov, *J. Phys. D* **33**, 2347 (2000).

¹⁴B. Anczykowski, D. Krüger, and H. Fuchs, *Phys. Rev. B* **53**, 15485 (1996).

¹⁵A. D. L. Humphris, J. Tamayo, and M. J. Miles, *Langmuir* **16**, 7891 (2000).

¹⁶M. Stark, R. W. Stark, W. M. Heckl, and R. Guckenberger, *Appl. Phys. Lett.* **77**, 3293 (2000).

¹⁷O. Sahin and A. Atalar, *Appl. Phys. Lett.* **79**, 4455 (2001).

¹⁸J. L. Hutter and J. Bechhoefer, *Rev. Sci. Instrum.* **64**, 1868 (1993).

¹⁹H. J. Butt and M. Jaschke, *Nanotechnology* **6**, 1 (1995).

²⁰N. A. Burnham, X. Chen, C. S. Hodges, G. A. Matei, E. J. Thoreson, C. J. Roberts, M. C. Davies, and S. J. B. Tendler, *Nanotechnology* **14**, 1 (2003).

²¹R. Proksch, T. E. Schaffer, J. P. Cleveland, R. C. Callahan, and M. B. Viani, *Nanotechnology* **15**, 1344 (2004).

²²J. P. Cleveland, S. Manne, D. Bocek, and P. K. Hansma, *Rev. Sci. Instrum.* **64**, 403 (1993).

²³J. E. Sader, J. W. M. Chon, and P. Mulvaney, *Rev. Sci. Instrum.* **70**, 3967 (1999).

²⁴A. Torii, M. Sasaki, K. Hane, and S. Okuma, *Meas. Sci. Technol.* **7**, 179 (1996).

²⁵C. T. Gibson, G. S. Watson, and S. Myhra, *Nanotechnology* **7**, 259 (1996).

²⁶P. J. Cumpson, P. Zhdan, and J. Hedley, *Ultramicroscopy* **100**, 241 (2004).

²⁷U. Rabe, K. Janser, and W. Arnold, *Rev. Sci. Instrum.* **67**, 3281 (1996).

²⁸M. P. Scherer, G. Frank, and A. W. Gummer, *J. Appl. Phys.* **88**, 2912 (2000).

²⁹R. W. Stark, G. Schitter, M. Stark, R. Guckenberger, and A. Stemmer, *Phys. Rev. B* **69**, 085412 (2004).

³⁰O. Sahin, C. F. Quate, O. Solgaard, and A. Atalar, *Phys. Rev. B* **69**, 165416 (2004).

³¹V. A. Spector and H. Flashner, *Trans. ASME, J. Dyn. Syst. Meas.* **112**, 186 (1990).

³²K. Yuan and L. Y. Liu, *J. Rob. Syst.* **20**, 581 (2003).

³³R. Arinero and G. Leveque, *Rev. Sci. Instrum.* **74**, 104 (2003).

³⁴T. E. Schäffer, *Nanotechnology* **16**, 664 (2005).

³⁵T. E. Schäffer and H. Fuchs, *J. Appl. Phys.* **97**, 083524 (2005).

³⁶R. W. Stark, *Rev. Sci. Instrum.* **75**, 5053 (2004).

³⁷A. Sebastian, M. V. Salapaka, D. J. Chen, and J. P. Cleveland, *J. Appl. Phys.* **89**, 6473 (2001).

³⁸F. J. Rubio-Sierra, R. Vazquez, and R. W. Stark, *Transfer Function Analysis of Atomic Force Microscope Cantilevers* (American Society of Mechanical Engineers, Orlando, FL, 2005).